



Cite this: *Phys. Chem. Chem. Phys.*,  
2018, **20**, 10100

Received 22nd January 2018,  
Accepted 21st March 2018

DOI: 10.1039/c8cp00481a

rsc.li/pccp

## Molecular dynamics study of the LCST transition in aqueous poly(*N*-*n*-propylacrylamide)

Tiago E. de Oliveira, <sup>a</sup> Carlos M. Marques <sup>a</sup> and Paulo A. Netz <sup>b</sup>

The breadth of technological applications of smart polymers relies on the possibility of tuning their molecular structure to respond to external stimuli. In this context, *N*-substituted acrylamide-based polymers are widely studied thermoresponsive polymers. Poly(*N*-*n*-propylacrylamide) (PNnPAm), which is a structural isomer of the poly(*N*-isopropylacrylamide) (PNIPAm) exhibits however, a lower phase transition in aqueous solution. In this work, we use all-atom molecular dynamics simulations of PNnPAm in aqueous solutions to study, from a microscopic point-of-view, the influence of chain size and concentration on the LCST of PNnPAm. Our analysis shows that the collapse of a single oligomer of PNnPAm upon heating is dependent on the chain length and corresponds to a complex interplay between hydration and intermolecular interactions. Analysis of systems with multiple chains shows an aggregation of PNnPAm chains above the LCST.

### Introduction

Thermoresponsive polymers exhibiting the coil-to-globule phase transition at the lower critical solution temperature (LCST) have attracted great interest in the development of new smart materials.<sup>1–7</sup> Several *N*-substituted acrylamide-based polymers exhibit a drastic phase transition by slight changes in temperature. Arguably the most extensively investigated poly-*N*-substituted acrylamide is poly(*N*-isopropylacrylamide) (PNIPAm), which displays a LCST at 305 K in water.<sup>1</sup> Poly(*N*-*n*-propylacrylamide) (PNnPAm), containing *n*-propyl groups as *N* substituents (Fig. 1), exhibits also a thermoresponsive behavior,<sup>8</sup> but a somewhat different phase behavior from PNIPAm: lower transition temperature (297 K)<sup>2,3</sup> and a more discontinuous transition with a steeper size change.<sup>3,4,9,10</sup>

Whereas all *N*-substituted acrylamide-based polymers present similar intramolecular (polymer–polymer) as well intermolecular (polymer–solvent) interactions, the details of these interactions, which are responsible for the differences in thermo-responsivity, depend of the structure of the monomeric units.

Experimentally, PNnPAm gels have been studied in water and their phase transition has been compared to that of PNIPAm gels.<sup>3,9,10</sup> In 1995, Komai *et al.*, have studied the volume phase transition of PNnPAm gels in water and in different aqueous alcohols and proposed that PNnPAm polymers are stiffer than PNIPAm.<sup>4</sup> Recently, it has been described that the LCST can be tuned by copolymerization of NnPAm with NIPAm,<sup>11,12</sup> NIPMAm<sup>11,13</sup> or *N*-ethylacrylamide (NEAm).<sup>8</sup> More recently,

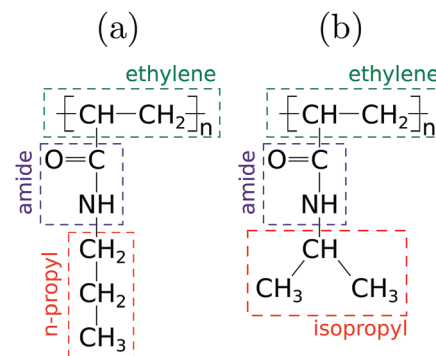


Fig. 1 A schematic representation of a PNnPAm (a) and PNIPAm (b) monomers.

Hellweg *et al.*, showed that the addition of anionic surfactants has a strong influence on the size of acrylamide-based microgels consisting of NnPAm.<sup>14</sup> Noticeably, since the hysteresis of PNnPAm is more pronounced than that of PNIPAm, co-polymerization of the two monomers allows also to tune the hysteresis of the transition.<sup>8,12,15</sup> This hysteresis can be considered as a strong indication that the transition, which occurs in acrylamide-based polymers (*e.g.* PNIPAm and PNnPAm), is likely a first-order transition.<sup>16</sup>

Despite the many studies devoted to the understanding of the phase transition of *N*-substituted acrylamide-based polymers, the role played by the molecular structure of the side chains (*e.g.* *n*-propyl *versus* isopropyl) is still an open question. In this context, molecular dynamics simulations (MD) can provide detailed information on the interaction generated by the different molecular groups. In 2011, Pang *et al.*, have used MD simulations

<sup>a</sup> Institut Charles Sadron, Université de Strasbourg, CNRS, Strasbourg, France.

E-mail: tiago.espinosa@ics-cnrs.unistra.fr

<sup>b</sup> Universidade Federal do Rio Grande do Sul, Porto Alegre, Brazil

and quantum calculations to study monomers units and short oligomers of NnPAm, NIPAm and NIPMAm in aqueous solution, comparing the effect of *n*-propyl and isopropyl groups on the monomer–monomer and monomer–water interactions. According to these authors, the presence of *n*-propyl group yields a less structured first solvation shell and stronger monomer–monomer interactions, allowing for closer contacts between NnPAm monomers, thus decreasing the LCST.<sup>17</sup>

In the present work, we employ all-atom MD simulations to understand the detailed mechanism behind the temperature-induced collapse of PNnPAm oligomers and short polymers in water, inspecting in particular the effect of temperature on the hydration structure and dynamics. We study the influence of the number of monomers and polymer concentration on the chains structural and dynamical behavior. Simulations of single-chain oligomers of PNnPAm from 4 to 32-mers were carried out at 280, 290, 300, 310, 320 and 340 K to understand the changes in the radius of gyration induced by the coil-to-globule transition of PNnPAm below and above the LCST. In addition to a single chain of PNnPAm molecule with 32-mers units, we have also investigated a system containing 4 chains of 32-mers.

## Simulation methods and models

### Force field

In order to investigate the coil-to-globule transition, we have used an all-atom model of PNnPAm and water. The choice of an appropriate force field determines the accuracy of the MD simulations. We have used OPLS-AA (Optimized Potentials for Liquid Simulations) force field<sup>18</sup> to describe PNnPAm<sup>19–25</sup> parameters combined with the SPC/E water model.<sup>26</sup>

The structure of a NnPAm monomer (see Fig. 1) was generated and optimized with a semi-empirical AM1<sup>27</sup> calculation using GAUSSIAN.<sup>28</sup> After that the monomer was repeated to generate chains with four different chain lengths (4, 8, 16 and 32-mers), controlling the stereochemistry to obtain atactic structures since it is known that tacticity can affect the LCST transition in PNIPAm,<sup>24</sup> a polymer with a closely related structure. The topology construction followed the GROMOS' logic of building blocks,<sup>29</sup> being in this way readily adaptable to other simulation conditions such as larger chains.

### Molecular dynamics simulation details

Six different systems were generated placing the polymer chains in a cubic box according to Table 1. These chains were equilibrated for 50 ps followed by solvation with SPC/E water molecules.<sup>26</sup> Simulations were then carried out in triplicate for 50 ns at each temperature. Only the last 25 ns were considered as the production run for all dynamical analysis. Information about the systems is listed in Table 1. This simulation time is larger than the structural relaxation time  $\tau \sim 4$  ns for a PNnPAm chain with 32-mers in pure water at 280 K.<sup>†</sup> Moreover,

<sup>†</sup>  $\tau$  was estimated using the end-to-end auto-correlation function ( $\langle R_{ee}(t) \cdot R_{ee}(0) \rangle \propto e^{-t/\tau}$ ), where  $R_{ee}(t)$  is the end-to-end vector of the chain.

**Table 1** System details applied in this study. The number of chains  $N_{\text{chains}}$ , number of monomer units per chain  $N_{\text{mers}}$ , the size of the side box  $l$ , the temperature range of simulations  $T_{\text{range}}$  and the simulation time

System	$N_{\text{chains}}$	$N_{\text{mers}}$	$N_w$	$l$ (nm)	$T_{\text{range}}$ (K)	$t$ (ns)
a	1	4	2151	4	280, 290, 300, 310, 320 and 340	50
b	1	8	4086	5	280, 290, 300, 310, 320 and 340	50
c	1	16	7041	6	280, 290, 300, 310, 320 and 340	50
d	1	32	15 000	8	280, 290, 300, 310, 320 and 340	50
e	1	32	15 000	8	280 and 340	250
f	4	32	60 000	12	280 and 340	50

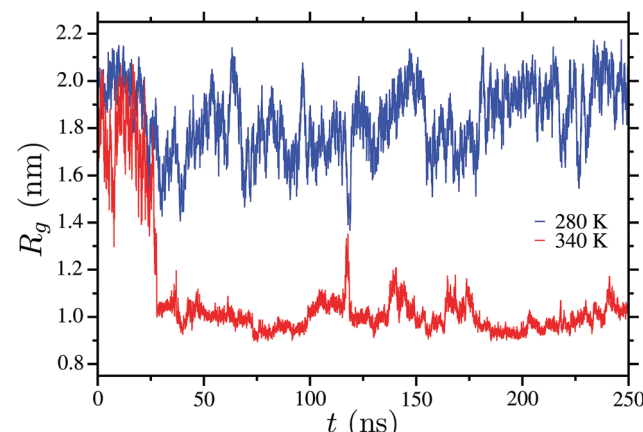


**Fig. 2** Time evolution of polymer radius of gyration  $R_g$  for PNnPAm at two different temperatures (280 and 340 K).

we have also performed simulations for 250 ns for a PNnPAm chain with  $N_{\text{mers}} = 32$  in pure water at 280 and 340 K to verify the stability of the extended and collapsed polymer structures (see Fig. 2).

The GROMACS-2016 package<sup>30</sup> was used to carry out all simulations. Simulations were conducted in *NPT* ensembles at ambient pressure (1 atm) using Berendsen barostat<sup>31</sup> and Velocity Rescaling thermostat.<sup>32</sup> The coupling constants for temperature ( $\tau_t$ ) and pressure ( $\tau_p$ ) are both equal to 0.5 ps. The leapfrog integration algorithm<sup>33</sup> with a 2 fs time step was employed. The systems described in Table 1 were constructed in cubic simulation boxes with periodic boundary conditions. All non-bonded interactions were treated with a cutoff of 1.2 nm and the long range electrostatic interactions were calculated using Particle Mesh Ewald.<sup>34</sup> Vibrations of bonds containing hydrogen atoms are constrained using a LINCS algorithm.<sup>35</sup> The trajectories were stored every 4 ps.

Based on the trajectories generated by the simulations, several quantities were calculated taking into account only the last 25 ns of each simulation, related to the oligomers structure (radius of gyration  $R_g$ <sup>36</sup>), persistence length ( $\ell_p$ )<sup>37,38</sup> and solvent accessible surface,<sup>36</sup> and also related to oligomer–water interactions and in their structural aspects (radial distribution function  $g(r)$ ,<sup>30,36</sup> water coordination number, H-Bond pattern<sup>30,36,39</sup>).

## Results and discussions

### Single chain in water

**Global structure of the polymer chain.** Considering the experimentally known coil-to-globule transition of PNnPAm at about 297 K, it is expected that the dimensions of the oligomers decrease with increasing temperature, showing a global structural transition. Fig. 3 shows the structure of PNnPAm 32-mers after 50 ns of simulation time, at 280 and 340 K.

In Fig. 3(a) the polymer is in a coil state at 280 K after 50 ns and in Fig. 3(b) at 340 K it is in a globule state. The polymer has therefore undergone a coil-to-globule transition as the temperature was increased. The structural changes for PNnPAm oligomers with different chain lengths (4, 8, 16 and 32-mers) are shown in terms of gyration radii ( $R_g$ ) (averaged over the last 25 ns of the simulations and over all replicas) in Fig. 4. The  $R_g$  for short oligomers of PNnPAm (4, 8, 16-mers) fluctuates around the mean value of  $R_g$  for each chain length, with roughly the same value, irrespective of temperature. For example, for oligomers with short chain length, such as 8-mers,  $R_g$  is equal to 0.66 nm with a deviation of 0.04 below and above the LCST. Therefore, oligomers with 4, 8 and 16-mers do not present a phase transition, the chain length being too short so that the oligomer is not able to fold. On the other hand, increasing the number of monomers to 32 we find that there is a clear difference in  $R_g$  at lower and high temperatures (Fig. 4 – blue stars) which indicates a coil-to-globule phase transition in PNnPAm between 290 and 300 K.

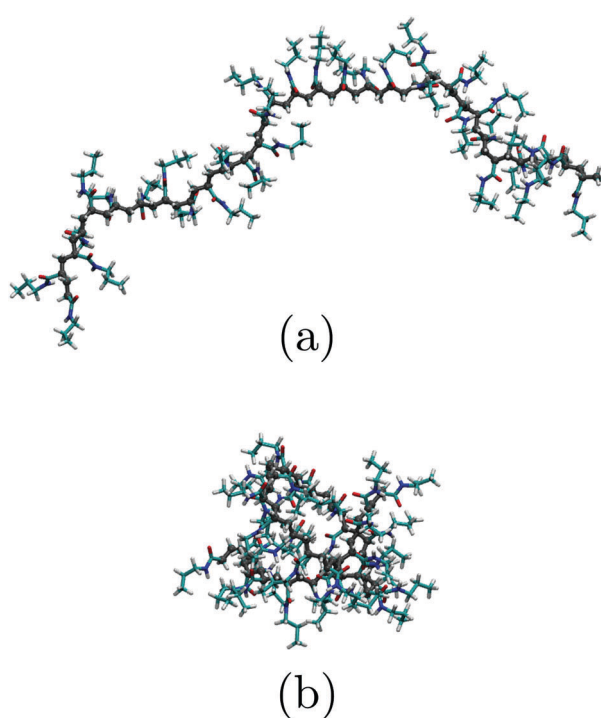


Fig. 3 Snapshot of a PNnPAm chain for 32-mers at the end of 50 ns at two different temperatures: (a) below the LCST (280 K) and (b) above the LCST (340 K). The carbon backbone atoms are shown in gray and water molecules have been omitted for clarity.

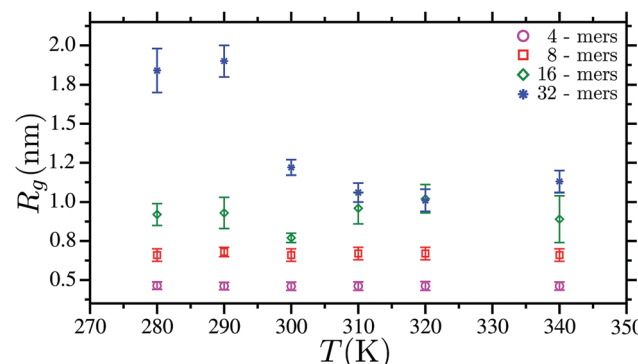


Fig. 4 Gyration radii  $R_g$  of a PNnPAm chain of length  $N = 32$  as a function of temperature for four chains with different chain lengths (4, 8, 16 and 32-mers).

Comparing with our previous work on PNIPAm,<sup>24</sup> in Fig. 5 we fit the radius of gyration ( $R_g$ ) using a Boltzmann sigmoid function:<sup>40</sup>

$$R_g(T) = R_g^{\text{expanded}} - \frac{(R_g^{\text{expanded}} - R_g^{\text{collapsed}})}{1 + \exp\left(\frac{T - T_c}{\Delta T}\right)}, \quad (1)$$

where  $T_c$  is the transition temperature and  $\Delta T$  the transition width. Here, we found  $T_c = 296$  K for PNnPAm and  $T_c = 302$  K to PNIPAm, these temperatures being in good agreement with the experimental observation for both polymers in aqueous solutions.<sup>3,4,9,10</sup> Furthermore, our  $\Delta T$  for both polymers is, approximately, 6 K, also in good quantitative agreement with the experimental data obtained from PNnPAm and PNIPAm in aqueous solutions.

In order to correlate the polymer collapse transition and its intrinsic rigidity we calculate the persistence length  $\ell_p$ . The persistence length is expressed in units of monomers. From our simulations, the calculation of the persistence length yielded 5 monomers for PNnPAm and in our previous results  $\ell_p$ , for

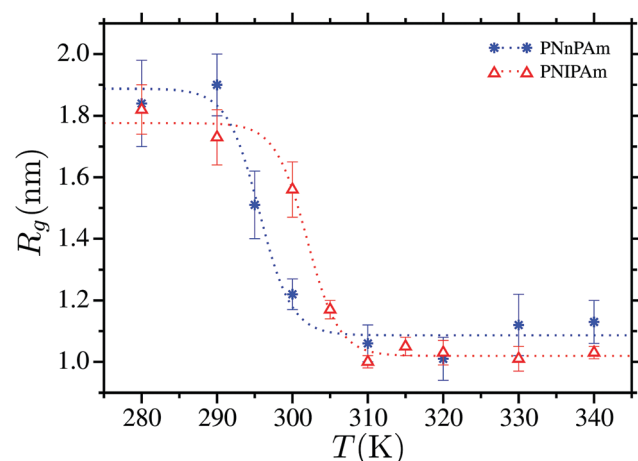


Fig. 5 Radius of gyration ( $R_g$ ) for PNnPAm and PNIPAm chains of length  $N = 32$  as a function of temperature. The dotted lines are fits based on eqn (1).

atactic PNIPAm, was found equal to 3 monomers. Differences in  $\ell_p$  must result from the difference between the side chains in PNnPAm and PNIPAm. In PNnPAm oligomers, the hydrophobic interactions between the *n*-propyl groups are enhanced resulting in a partial collapse of the chain and inducing an increased stiffness of the chain. Significantly, monitoring the number of hydrophobic contacts in both polymers, it can be found that not only PNIPAm has more contacts than PNnPAm (1543 against 1464) at 280 K, but also this number increases by 25% for PNnPAm (1464 contacts at 280 K and 1830 at 340 K) and by 20% for PNIPAm (1543 contacts at 280 K and 1848 at 340 K).

The results concerning the global structure also indicate that polymer shrinks with increasing temperature, decreasing the solvent accessible area. The detailed solvent structure around hydrophobic and hydrophylic moieties will be explored in the next section.

The solvent accessible surface (SAS) for a 32-mer also confirms the phase transition, as can be seen in Fig. 6, which shows the SAS as a function of the time. Since the transition involves the hydrophilic and hydrophobic parts of the monomer, the amount of accessible surface area to the water should decrease above the transition. The solvent accessible surfaces for hydrophilic and hydrophobic parts are reduced by 16% and 19%, respectively, with the increase of temperature from 280 K to 340 K (see Table 2). SAS data indicates that the structure of PNnPAm is collapsed and less exposed to water above the transition temperature. Both hydrophobic and hydrophilic SAS values, below the LCST, are higher for PNnPAm than for PNIPAm (see Table 2). The *n*-propyl side group allows a better exposition to water (see also the next section). Besides, upon increasing temperature, the hydrophobic SAS decreases much strongly for PNnPAm than for PNIPAm. As a result, the SAS decrease is stronger for PNnPAm than for PNIPAm, yielding a larger gain in translational entropy of water molecules. This entropy gain can be explained either by the release of a larger amount of water molecules upon heating in the case of PNnPAm or alternatively by the decrease of the solvent-excluded volume (see for instance Galamba<sup>41</sup> and Graziano<sup>42</sup>).

**Hydration and solvent structure.** The radial distribution function  $g(r)$  can be used to investigate the structure of solvent located close to the chain. The structural changes in solvent molecules within the hydration shell play an important role on the LCST and in the polymer conformation. Therefore, we calculate  $g(r)$  for the center-of-mass (COM) of amide group with the water COM ( $g(r)^{aw}$ ) and the COM of the *n*-propyl group with water COM ( $g(r)^{npw}$ ) for the side chain and also for the COM of ethylene group (chain backbone) with water COM ( $g(r)^{bw}$ ). To investigate the hydration we calculate the coordination number of water molecules around a given group  $\alpha$  ( $N_{\alpha w}$ ,  $\alpha = a, np, b$ ), as follows:

$$N_{\alpha w} = 4\pi\rho \int_0^{r_0} g(r)^{\alpha w} r^2 dr. \quad (2)$$

Here  $r_0$  is the range of the 1st and 2nd solvation shell. Results of  $g(r)$  between different polymer segments and solvent molecules are shown in Fig. 7. The structure of water around the

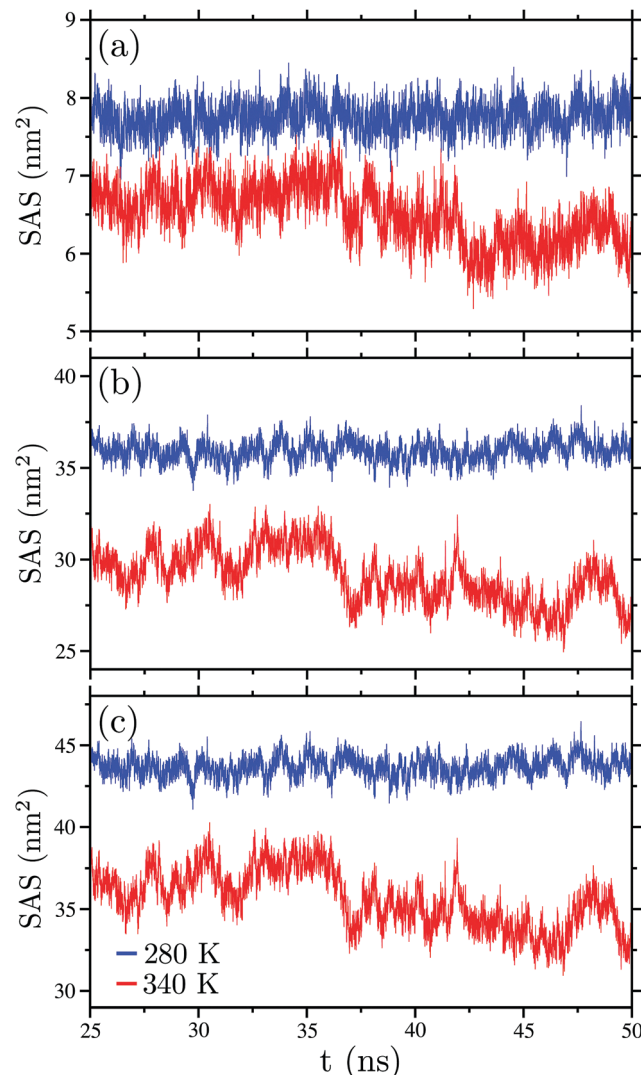


Fig. 6 Evolution of the (a) hydrophilic, (b) hydrophobic and (c) total solvent accessible surface (SAS) during the last 25 ns of simulation.

Table 2 Solvent accessible surface area (SAS) for 32-mers of PNnPAm and PNIPAm<sup>24</sup> for different temperatures  $T$

$T$ (K)	SAS (nm <sup>2</sup> )					
	Hydrophilic		Hydrophobic		Total	
	PNnPAm	PNIPAm	PNnPAm	PNIPAm	PNnPAm	PNIPAm
280	7.76	6.59	35.94	34.77	43.70	41.36
340	6.50	5.95	29.11	31.71	35.61	37.66

hydrophilic part of PNnPAm is shown in Fig. 7(a), where we can see that the height of the first minimum ( $\sim 0.44$  nm) decreases with the increase of the temperature, whereas between 0.5 and 1.25 nm the changes are even more significant, with the shoulders corresponding to the second and third hydration shells almost disappearing at the highest temperature. The water coordination number  $N_{aw}$  in PNnPAm (3.8 and 2.8, below and above the LCST, respectively, see Table 3) is higher than in PNIPAm (1.55 and 1.28, below and above the LCST,

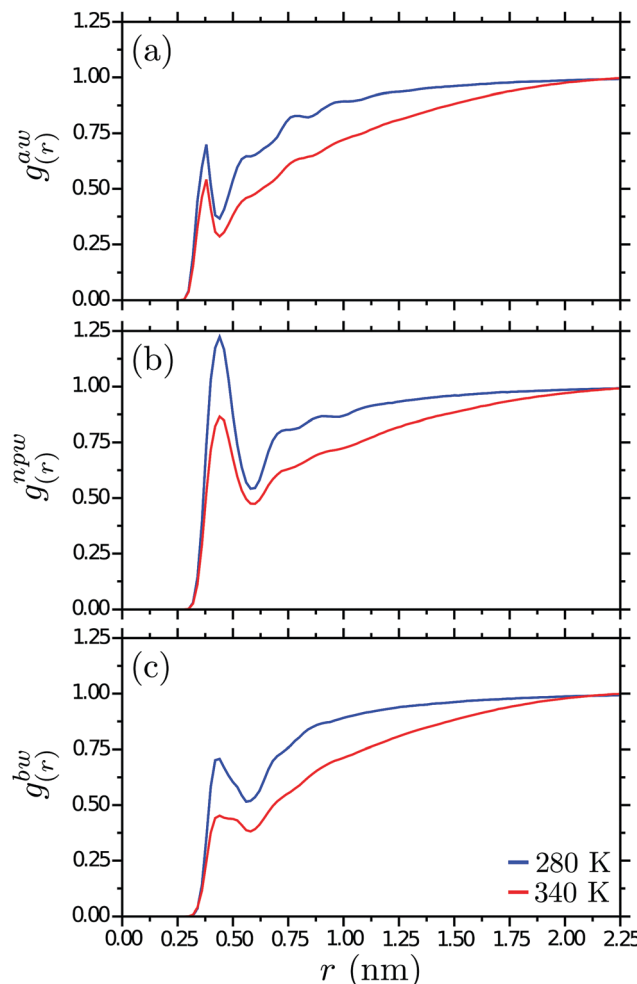


Fig. 7 Radial distribution between (a) amide moieties and water molecules ( $g(r)^{aw}$ ); (b) *n*-propyl moieties and water molecules ( $g(r)^{npw}$ ); (c) ethylene moieties and water molecules ( $g(r)^{bw}$ ), as a function of two different temperatures.

Table 3 Water coordination number around the groups amide ( $N_{aw}$ ), *n*-propyl ( $N_{npw}$ ) and ethylene ( $N_{bw}$ )

Hyd. shell	$N_{aw}$		$N_{npw}$		$N_{bw}$	
	280 K	340 K	280 K	340 K	280 K	340 K
1st	3.8	2.8	18.0	13.2	10.5	7.1
2nd	16.0	10.0	50.5	38.1	31.1	21.5

respectively) Also the decrease in  $N_{aw}$  with heating ( $\sim 26\%$ ) is stronger in PNnPAm.<sup>24</sup> The linear structure of the *n*-propyl group of PNnPAm enables a better access of water to the amide group compared to the case of PNIPAm.

Inspecting the structure of water around the hydrophobic regions of the *n*-propyl (side chain) and ethylene (backbone), we notice that the first minimum in  $g(r)^{npw}$  and  $g(r)^{bw}$  are  $\sim 0.58$  and  $\sim 0.56$  nm, respectively. In both cases the  $g(r)$  follows the same trend regarding the temperature, as shown in Fig. 7(b) and (c). However in Fig. 7(b) for the first and second hydration shells the structure of solvent also decreases with the

temperature and  $N_{npw}$  decreases by  $\sim 27\%$  for the first hydration shell and  $\sim 25\%$  in the second. For the case shown in Fig. 7(c), in the first and second hydration shell  $N_{bw}$  decreases by  $\sim 33\%$  and  $\sim 31\%$ , respectively. Furthermore, the  $N_{npw}$  shows that the side chains of the PNnPAm are significantly more exposed to water than the isopropyl group of PNIPAm. Indeed, the water coordination number around the isopropyl group (PNIPAm) is 13.50 and 11.33 water molecules at 280 and 340 K, respectively,<sup>24</sup> while  $N_{npw}$  values for PNnPAm, at temperatures below and above the LCST are 18.0 and 13.2 water molecules, respectively (Table 3). Notice that the hydration changes upon heating are more pronounced for PNnPAm compared to PNIPAm.

On the other hand, the intramolecular interactions become stronger upon increasing temperature, seen from the increase of the first and second peaks of the radial distribution function between the *n*-propyl moieties, the signature of the tendency to collapse the molecule by heating, as shown in Fig. 8.

In *N*-substituted acrylamide-based polymers, the hydrogen bonds, despite not being the driving force of the collapse, play an important role in the coil-to-globule transition.<sup>43</sup> In the coil state, intermolecular hydrogen bonds between amide group and water are a key factor for the solubility of the polymer chain. The total number of hydrogen bonds between amide group and water ( $n_{hb}^{aw}$ ), decrease from 2.3 to 1.7 hydrogen bonds per monomer with the increase of temperature for PNnPAm and PNIPAm.<sup>24</sup> We analyzed also the individual contribution of each atom capable of forming hydrogen bonds in the amide group: oxygen (OAM), nitrogen (NAM) and hydrogen (HAM). In the case of PNnPAm, OAM has  $\sim 2.0$  hydrogen bond per monomer below the LCST and  $\sim 1.0$  hydrogen bond per monomer above the LCST. The contributions of the atoms NAM and HAM are less than 1.0 hydrogen bond per monomer. For PNIPAm, Deshmukh *et al.* in 2012,<sup>44,45</sup> obtain a similar pattern for the number of hydrogen bonds between PNIPAM amide group and water. For temperatures below the LCST the OAM is free to form two hydrogen bonds with water and above the LCST one of these bonds breaks to form one intramolecular hydrogen bond.

Regarding the intramolecular interactions, we analyzed the number of hydrogen bonds between amide moieties ( $n_{hb}^{aa}$ ).

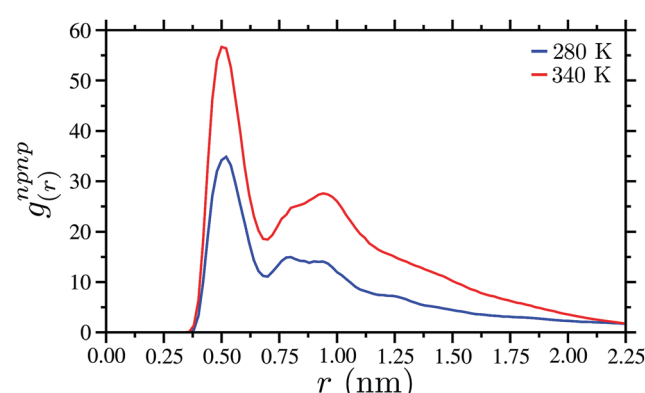


Fig. 8 Radial distribution between *n*-propyl moieties ( $g(r)^{npnp}$ ).

**Table 4** Number of hydrogen bonds between monomers located at different distances along the chain

T (K)	$n - [n + 1]$	$n - [n + 2]$	$n - [n + 3]$	$n - [n + 4]$	$n - [n + 5]$	$n - [n + x]; x > 6$	$n_{hb}^{aa}$
280	0.6	0.5	0.0	0.0	0.0	0.0	1.1
340	1.0	1.0	0.04	0.1	0.0	1.2	3.3

The average  $n_{hb}^{aa}$  per monomer as a function of temperature, below and above the LCST, are  $0.03 \pm 0.03$  and  $0.11 \pm 0.05$ , respectively. The total number of hydrogen bonds between monomers separated by given distances along the chain can be seen in Table 4. In this table, is shown the total (not the average per monomer) number of hydrogen bonds formed between adjacent residues ( $n - [n + 1]$ ), separated by 1 ( $n - [n + 2]$ ), by 2 ( $n - [n + 3]$ ), by 3 ( $n - [n + 4]$ ), by 4 ( $n - [n + 5]$ ) or by more than 4 repeating monomers ( $n - [n + x]$ ;  $x > 6$ ). Consistently, we found, by analyzing the number of hydrogen bonds between monomers separated by given distances along the chain, that bonds between topologically close monomers are already formed below LCST and increase with the temperature, whereas the bonds between monomers located far apart appear only above LCST. Furthermore, it should also be mentioned that the  $n_{hb}^{aw}$  is not entirely compensated by the increase of the  $n_{hb}^{aa}$ . The total number of  $n_{hb}^{aa}$  for PNnPAm is higher with increasing temperature, 1.1 and 3.3 below and above the LCST, respectively. Simulations also reveal that comparable values are obtained for PNIPAm with 1.8 intra-molecular hydrogen bonds below the LCST (280 K) and 3.1 intra-molecular hydrogen bonds above the LCST (340 K). Despite the larger variations upon collapse in the water coordination number around the PNnPAm and PNIPAm due to the slight differences in the side groups of these polymers, the intra-molecular hydrogen bond pattern is similar for both polymers.

### Multiple chains in water

As a first attempt to understand the shrinkage of a microgel, we examined the influence of the number of PNnPAm chains in water, as described in Table 1.

Under our conditions, one would expect aggregation of the chains above the LCST. As Fig. 9 shows, this is indeed what can be observed for a system with 4 oligomers of 32-mers, after 50 ns. Below the LCST (280 K) the chains are well dispersed in the solution, forming aggregates above the LCST (340 K).

As the data in Table 5 shows, all the chains display, above the LCST,  $R_g$  values comparable to those of individually collapsed chains. The aggregate of chains above the LCST can therefore be viewed as a globule of collapsed chains.

We have calculated the number of inter-chains contacts (NC) in a distance of 0.6 nm, to measure the inter-chains interactions among the oligomers. NC increases with the temperature, below the LCST, NC is equal to 912 contacts per chain while 3643 contacts per chain are found above the LCST. This increase of ~300% of NC is consistent with the formation of a shrunk physical gel.

As in the case of single chains in aqueous solution, we investigate the water coordination number around the oligomers. For the system of 4 × 32-mers the number of water

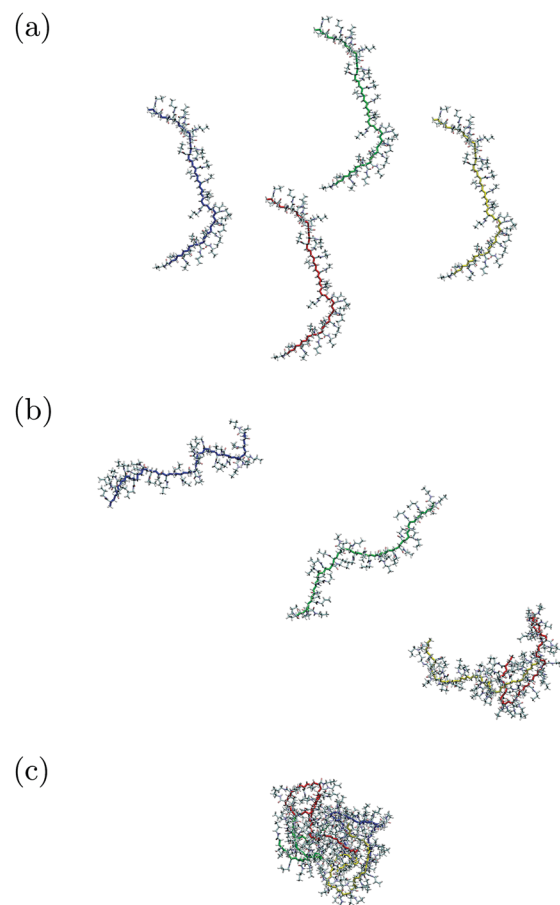


**Fig. 9** Snapshot of multiple chains of PNnPAm in aqueous solution, initial configuration (a) and final structure of the system 4 × 32-mers below (280 K) (b) and above (340 K) (c) the LCST.

**Table 5** Gyration radii  $R_g$  (in nm) for each chain in the system for two different temperatures

Chains	4 × 32-mers	
	280 K	340 K
1	$1.95 \pm 0.09$	$1.12 \pm 0.02$
2	$1.79 \pm 0.13$	$1.13 \pm 0.03$
3	$1.77 \pm 0.18$	$0.93 \pm 0.02$
4	$1.81 \pm 0.16$	$1.02 \pm 0.03$

molecules around the amide, *n*-propyl and ethylene groups ( $N_{aw}$ ,  $N_{npw}$  and  $N_{bw}$ ) decreases by 33.5%, 37.6% and 42.7%, respectively when the temperature is increased. On the other hand, the number of hydrophobic contacts between *n*-propyl/*n*-propyl, *n*-propyl/ethylene and ethylene/ethylene increases by 34.9%, 38.5% and 9.4%, respectively, when the temperature is increased (see Table 6). In this context, we calculate also the

**Table 6** Number of hydrophobic contacts between *n*-propyl/*n*-propyl, *n*-propyl/ethylene and ethylene/ethylene for two different temperatures

Contacts	280 K	340 K
<i>n</i> -Propyl/ <i>n</i> -propyl	2630 ± 101	3548 ± 160
<i>n</i> -Propyl/ethylene	1814 ± 45	2512 ± 57
Ethylene/ethylene	2390 ± 50	2614 ± 52

**Table 7** Intra-chain and inter-chain hydrogen bonds calculated between amide groups of PNnPAm as a function of two different temperatures

Hydrogen bonds	280 K	340 K
Intra-chain	1.34 ± 0.52	3.64 ± 2.20
Inter-chain	6.90 ± 0.77	20.50 ± 3.30

number of intra-chain and inter-chain hydrogen bonds between the amide groups (Table 7). For the case of intra-chain hydrogen bonds between amide groups the behavior is similar to intramolecular hydrogen bonds ( $n_{hb}^{aa}$ ) for the single chains, the number of intra-chain hydrogen bonds increasing by a factor two when the temperature is rised above the LCST. Due to the intimate contact between different chains in the globule, the number of inter-chain hydrogen bonds between amide groups increase also strongly (by a factor three) as the temperature is increased above the LCST.

## Conclusions

In this work, we have performed molecular dynamics simulations to investigate phase transition behavior of PNnPAm in aqueous solutions. We studied the influence of chain length by considering four different chains with 4, 8, 16 and 32 monomers. We have also studied the influence of the concentration of chains on the phase transition of PNnPAm, setting a simulation with 4 chains of 32 monomers in aqueous solution.

Our results clearly show that the coil-to-globule transition can only be observed for large enough chains. In our case the transition was not observed for oligomers with 16 monomers or less over the simulated range of temperatures. For the case with 32 monomers, PNnPAm undergoes a phase transition (coil-to-globule) above 290 K. We find that chains with 32 monomers are in a swollen coil state for  $T < 290$  K and assume a collapsed state for  $T > 300$  K. We now speculate on the reasons for PNnPAm collapse at a lower temperature than the closely related PNIPAm. A closer look at the hydrogen bonds between amide group and water reveals that the interaction with the amide group is qualitatively similar for both cases, but PNnPAm shows a higher water coordination and a stronger temperature-dependence. Besides, while looking into the hydrophobic capping of both monomers, it became clear that the hydrophobic part of PNnPAm has a larger water coordination number around the hydrophobic side chain than PNIPAm. We found that the water coordination around the hydrophobic side chain and also the solvent accessible surface both display a stronger decrease with the temperature for PNnPAm than for PNIPAm. As a consequence,

the translational entropy of water molecules displays a stronger increase (and at lower temperatures) for PNnPAm. This entropic effect linked to the hydrophobic hydration can be described as a consequence of a release of water from the hydration shell to the bulk or alternatively as a result of the solvent-excluded volume effect, related to the creation of a cavity in the solvent.<sup>42,46</sup> Therefore the increase of entropy is more pronounced in the case of PNnPAm, yielding a spontaneous collapsing at lower temperatures. In other words, the larger difference in the water coordination number around the hydrophobic side chain induces a stronger hydrophobic interaction and therefore initiates the collapse at a smaller  $T$  value ad a lower LCST. We are, of course, supposing that the enthalpic effects (originated by the hydrogen bonds) are comparable in both cases.

For the multiple chains systems we find a collective effect above the LCST (340 K). The  $R_g$  of chains show pronounced changes over the temperature range and the number of contacts (NC) of *n*-propyl moieties and the coordination number of water molecules around the oligomers changes drastically with the increase of temperature. In this case we have observed the aggregation of PNnPAm chains with the increase of the temperature.

## Conflicts of interest

There are no conflicts to declare.

## Acknowledgements

We thank Debashish Mukherji for many stimulating discussions and Thomas Hellweg for bringing ref. 9 and 12 to our attention. T. E. O. acknowledges hospitality at the Institut Charles Sadron where this work was performed. We thank Tobias Espinosa de Oliveira and Luis Andre Baptista for the critical reading of the manuscript. Simulation snapshots in this manuscript are rendered using VMD.<sup>47</sup>

## References

- 1 H. Schild, *Prog. Polym. Sci.*, 1992, **17**, 163–249.
- 2 M. Kano and E. Kokufuta, *Langmuir*, 2009, **25**, 8649–8655.
- 3 H. Inomata, S. Goto and S. Saito, *Macromolecules*, 1990, **23**, 4887–4888.
- 4 H. Kawasaki, T. Nakamura, K. Miyamoto, M. Tokita and T. Komai, *J. Chem. Phys.*, 1995, **103**, 6241–6247.
- 5 D. Mukherji, C. M. Marques and K. Kremer, *Nat. Commun.*, 2014, **5**, 4882.
- 6 S. Samanta, D. R. Bogdanowicz, H. H. Lu and J. T. Koberstein, *Macromolecules*, 2016, **49**, 1858–1864.
- 7 C. C. D. Silva, P. Leophairatana, T. Ohkuma, J. T. Koberstein, K. Kremer and D. Mukherji, *J. Chem. Phys.*, 2017, **147**, 064904.
- 8 T. Hirano, A. Ono, H. Yamamoto, T. Mori, Y. Maeda, M. Oshimura and K. Ute, *Polymer*, 2013, **54**, 5601–5608.
- 9 D. Ito and K. Kubota, *Macromolecules*, 1997, **30**, 7828–7834.

- 10 B. Wedel, Y. Hertle, O. Wrede, J. Bookhold and T. Hellweg, *Polymers*, 2016, **8**, 1–21.
- 11 K. Iwai, Y. Matsumura, S. Uchiyama and A. P. de Silva, *J. Mater. Chem.*, 2005, **15**, 2796–2800.
- 12 T. Hirano, H. Yamamoto and K. Ute, *Polymer*, 2011, **52**, 5277–5281.
- 13 M. Zeiser, I. Freudensprung and T. Hellweg, *Polymer*, 2012, **53**, 6096–6101.
- 14 B. Wedel, T. Brändel, J. Bookhold and T. Hellweg, *ACS Omega*, 2017, **2**, 84–90.
- 15 T. Hirano, K. Nakamura, T. Kamikubo, S. Ishii, K. Tani, T. Mori and T. Sato, *J. Polym. Sci., Part A: Polym. Chem.*, 2008, **46**, 4575–4583.
- 16 D. Mukherji, M. Wagner, M. D. Watson, S. Winzen, T. E. de Oliveira, C. M. Marques and K. Kremer, *Soft Matter*, 2017, **13**, 2292–2294.
- 17 J. Pang, H. Yang, J. Ma and R. Cheng, *J. Theor. Comput. Chem.*, 2011, **10**, 359–370.
- 18 W. L. Jorgensen, D. S. Maxwell and J. Tirado-Rives, *J. Am. Chem. Soc.*, 1996, **118**, 11225–11236.
- 19 J. Walter, V. Ermatchkov, J. Vrabec and H. Hasse, *Fluid Phase Equilib.*, 2010, **296**, 164–172.
- 20 J. Walter, J. Sehrt, J. Vrabec and H. Hasse, *J. Phys. Chem. B*, 2012, **116**, 5251–5259.
- 21 D. Mukherji and K. Kremer, *Macromolecules*, 2013, **46**, 9158–9163.
- 22 T. E. de Oliveira, P. A. Netz, D. Mukherji and K. Kremer, *Soft Matter*, 2015, **11**, 8599–8604.
- 23 D. Mukherji, M. Wagner, M. D. Watson, S. Winzen, T. E. de Oliveira, C. M. Marques and K. Kremer, *Soft Matter*, 2016, **12**, 7995–8003.
- 24 T. E. de Oliveira, D. Mukherji, K. Kremer and P. A. Netz, *J. Chem. Phys.*, 2017, **146**, 034904.
- 25 A. K. Tucker and M. J. Stevens, *Macromolecules*, 2012, **45**, 6697–6703.
- 26 H. J. C. Berendsen, J. R. Grigera and T. P. Straatsma, *J. Phys. Chem.*, 1987, **91**, 6269–6271.
- 27 M. J. S. Dewar, E. G. Zoebisch, E. F. Healy and J. J. P. Stewart, *J. Am. Chem. Soc.*, 1985, **107**, 3902–3909.
- 28 M. J. Frisch, G. W. Trucks, H. B. Schlegel, G. E. Scuseria, M. A. Robb, J. R. Cheeseman, J. A. Montgomery, Jr., T. Vreven, K. N. Kudin, J. C. Burant, J. M. Millam, S. S. Iyengar, J. Tomasi, V. Barone, B. Mennucci, M. Cossi, G. Scalmani, N. Rega, G. A. Petersson, H. Nakatsuji, M. Hada, M. Ehara, K. Toyota, R. Fukuda, J. Hasegawa, M. Ishida, T. Nakajima, Y. Honda, O. Kitao, H. Nakai, M. Klene, X. Li, J. E. Knox, H. P. Hratchian, J. B. Cross, V. Bakken, C. Adamo, J. Jaramillo, R. Gomperts, R. E. Stratmann, O. Yazyev, A. J. Austin, R. Cammi, C. Pomelli, J. W. Ochterski, P. Y. Ayala, K. Morokuma, G. A. Voth, P. Salvador, J. J. Dannenberg, V. G. Zakrzewski, S. Dapprich, A. D. Daniels, M. C. Strain, O. Farkas, D. K. Malick, A. D. Rabuck, K. Raghavachari, J. B. Foresman, J. V. Ortiz, Q. Cui, A. G. Baboul, S. Clifford, J. Cioslowski, B. B. Stefanov, G. Liu, A. Liashenko, P. Piskorz, I. Komaromi, R. L. Martin, D. J. Fox, T. Keith, M. A. Al-Laham, C. Y. Peng, A. Nanayakkara, M. Challacombe, P. M. W. Gill, B. Johnson, W. Chen, M. W. Wong, C. Gonzalez and J. A. Pople, *Gaussian 09*, Gaussian, Inc., Wallingford, CT, 2009.
- 29 W. F. van Gunsteren, S. R. Billeter, A. A. Eising, P. H. Hünenberger, P. Krüger, A. E. Mark, W. R. P. Scott and I. G. Tironi, *vdf Hochschulverlag AG an der ETH Zürich and BIOMOS b.v.*, Zürich, 1996.
- 30 S. Pronk, S. Páll, R. Schulz, P. Larsson, P. Bjelkmar, R. Apostolov, M. R. Shirts, J. C. Smith, P. M. Kasson, D. van der Spoel, B. Hess and E. Lindahl, *Bioinformatics*, 2013, **29**, 845–854.
- 31 H. J. C. Berendsen, J. P. M. Postma, W. F. van Gunsteren, A. DiNola and J. R. Haak, *J. Chem. Phys.*, 1984, **81**, 3684–3690.
- 32 G. Bussi, D. Donadio and M. Parrinello, *J. Chem. Phys.*, 2007, **126**, 014101.
- 33 R. W. Hockney, *Methods Comput. Phys.*, 1970, **9**, 135–211.
- 34 U. Essmann, L. Perera, M. L. Berkowitz, T. Darden, H. Lee and L. G. Pedersen, *J. Chem. Phys.*, 1995, **103**, 8577–8593.
- 35 B. Hess, H. Bekker, H. J. C. Berendsen and J. G. E. M. Fraaije, *J. Comput. Chem.*, 1997, **18**, 1463–1472.
- 36 M. Abraham, D. van der Spoel, E. Lindahl, B. Hess and the GROMACS development team, *GROMACS User Manual version 2016.2*.
- 37 L. M. J. Kroon-Batenburg, P. H. Kruiskamp, J. F. G. Vliegenthart and J. Kroon, *J. Phys. Chem. B*, 1997, **101**, 8454–8459.
- 38 J. Gross, M. Ivanov and W. Janke, *J. Phys.: Conf. Ser.*, 2016, **750**, 012009.
- 39 A. Luzar and D. Chandler, *J. Chem. Phys.*, 1993, **98**, 8160–8173.
- 40 D. J. Finney, *Int. Stat. Rev.*, 1979, **47**, 1–12.
- 41 N. Galamba, *J. Phys. Chem. B*, 2013, **117**, 2153–2159.
- 42 G. Graziano, *J. Phys. Chem. B*, 2014, **118**, 2598–2599.
- 43 Y. Maeda and M. Yamabe, *Polymer*, 2009, **50**, 519–523.
- 44 S. A. Deshmukh, S. K. R. S. Sankaranarayanan and D. C. Mancini, *J. Phys. Chem. B*, 2012, **116**, 5501–5515.
- 45 S. A. Deshmukh, S. K. R. S. Sankaranarayanan, K. Suthar and D. C. Mancini, *J. Phys. Chem. B*, 2012, **116**, 2651–2663.
- 46 A. Pica and G. Graziano, *Phys. Chem. Chem. Phys.*, 2015, **17**, 27750–27757.
- 47 W. Humphrey, A. Dalke and K. Schulten, *J. Mol. Graphics*, 1996, **14**, 33–38.